https://ntrs.nasa.gov/search.jsp?R=19660006995 2020-03-16T23:13:22+00:00Z

AD621375

THE PENNSYLVANIA
STATE UNIVERSITY

IONOSPHERIC RESEARCH

Scientific Report No. 247

A SUBSONIC D-REGION PROBE-THEORY AND INSTRUMENTATION

CLEARINGHOUSE
FOR FEDERAL SCIENTIFIC AND
TECHNICAL INFORMATION
Hardcopy | Microfiche
$2.00 | $0.75 | 48 pp
ARCHIVE COPY

by
L. C. Hale and D. P. Hou

August 31, 1965

The research reported in this document has been supported by the Army Research Office-Durham under Grant DA-ARO-D-31-124-G659 and, in part, by the National Aeronautics and Space Administration under Grant NsG-134-61.

IONOSPHERE RESEARCH LABORATORY

SEP 21 1965
CLEARINGHOUSE
FOR FEDERAL SCIENTIFIC AND
TECHNICAL INFORMATION

University Park, Pennsylvania

ARO Grant DA-ARO-D-31-124-G659

Ionospheric Research

ARO Grant DA-ARO-D-31-124-G659

Scientific Report

on

A Subsonic D-Region Probe-Theory and Instrumentation

by

L. C. Hale and D. P. Hoult

August 31, 1965

Scientific Report No. 247

"The research reported in this document has been supported by the Army Research Office-Durham under Grant DA-ARO-D-31-124-G659 and, in part, by the National Aeronautics and Space Administration under Grant NsG-134-61."

Submitted by:

L. C. Hale (and)

L. C. Hale, Assistant Professor of Electrical Engineering

John S Nisbet (and)

J. S. Nisbet, Associate Professor of Electrical Engineering

Approved by:

A. H. Waynick, Director, Ionosphere Research Laboratory

Ionosphere Research Laboratory

The Pennsylvania State University

College of Engineering

Department of Electrical Engineering

Table of Contents

16284

ABSTRACT

The philosophy, theory, and a description of the instrumentation of a subsonic, D-region ion and electron probe are presented. It is shown theoretically that a blunt, high potential, parachute borne probe collects charged particles according to a simple, angle of attack independent, mobility theory. This theory has been substantiated experimentally with payloads launched on Arcas rockets. The design of these payloads, which include a range-switching electrometer and low-cost telemetry system, is discussed in detail.

Author

I. Introduction

This report describes a rocket launched, parachute borne probe system for the measurement of positive ion and electron densities in the 30 to 80 km. altitude range.

Ground based and rocket borne radio propagation experiments are yielding a good picture of electrons in the upper part of this range in the daytime. However, in the lower part of this region, and throughout the region at night, electrons are thought to be small in number density compared to positive and negative ions. Hence a more complete understanding of the charged particle densities, and ultimately of the basic physical processes of the region require methods of determining positive and negative ion densities.

Hoult[1] (1964) has shown that even weak shock waves can introduce large uncertainties into measurements of charged particle densities with supersonic probes. Accordingly, it was decided to employ a parachute borne probe system in order to obtain subsonic velocities in the 30 to 80 km. altitude range. This parachute borne probe system is described in this report.

The basic philosophy of measurement and a description of the initial experiments are given. Appendix I, by D. P. Hoult, gives the basic theory governing the behavior of the probe in the D-region of the ionosphere. Appendix II, by L. C. Hale, describes the probe technology, including the rocket borne instrumentation, telemetry system, and ground based equipment.

II. Experimental Techniques

The vehicle chosen for this program was the Arcas meteorological

rocket, which is routinely used for wind and temperature measurements at the altitudes of interest with a parachute-borne payload. This system is of low cost, and has been proven capable of high reliability. The launchings are done in conjunction with the U. S. Army Electronics Research and Development Activity at White Sands Missile Range, New Mexico.

The probe used in the initial experiments is shown in Figure 1, which also shows an Arcas nose cone. The upper and somewhat smaller can contains the electronics associated with the probe and the telemetry transmitter and modulator, and battery power for the electronics associated with the experiment. The sleeve on the side of the can is a slot telemetry antenna, which was developed to provide an adequate radiation pattern, consistent with a clean geometry. The small disc in the top of the can is the probe collector. The rest of the can, operated at the same potential as the disc, serves as a "guard" electrode. The lower and larger can, which contains the batteries for the telemetry transmitter, is the other half of the bipolar probe, providing a return current path to the medium. The potential of the probe is varied by sweeping the potential of one can with respect to the other. The base plate at the very bottom of the probe assembly attaches to the parachute, so that the probe hangs inverted, thus exposing the probe surface to the streaming medium, and preventing sunlight from falling on the collecting disc. This is a necessary condition to prevent photoelectric currents from contaminating the data.

III. Probe Geometry

It is desirable to have a probe system that can be thoroughly

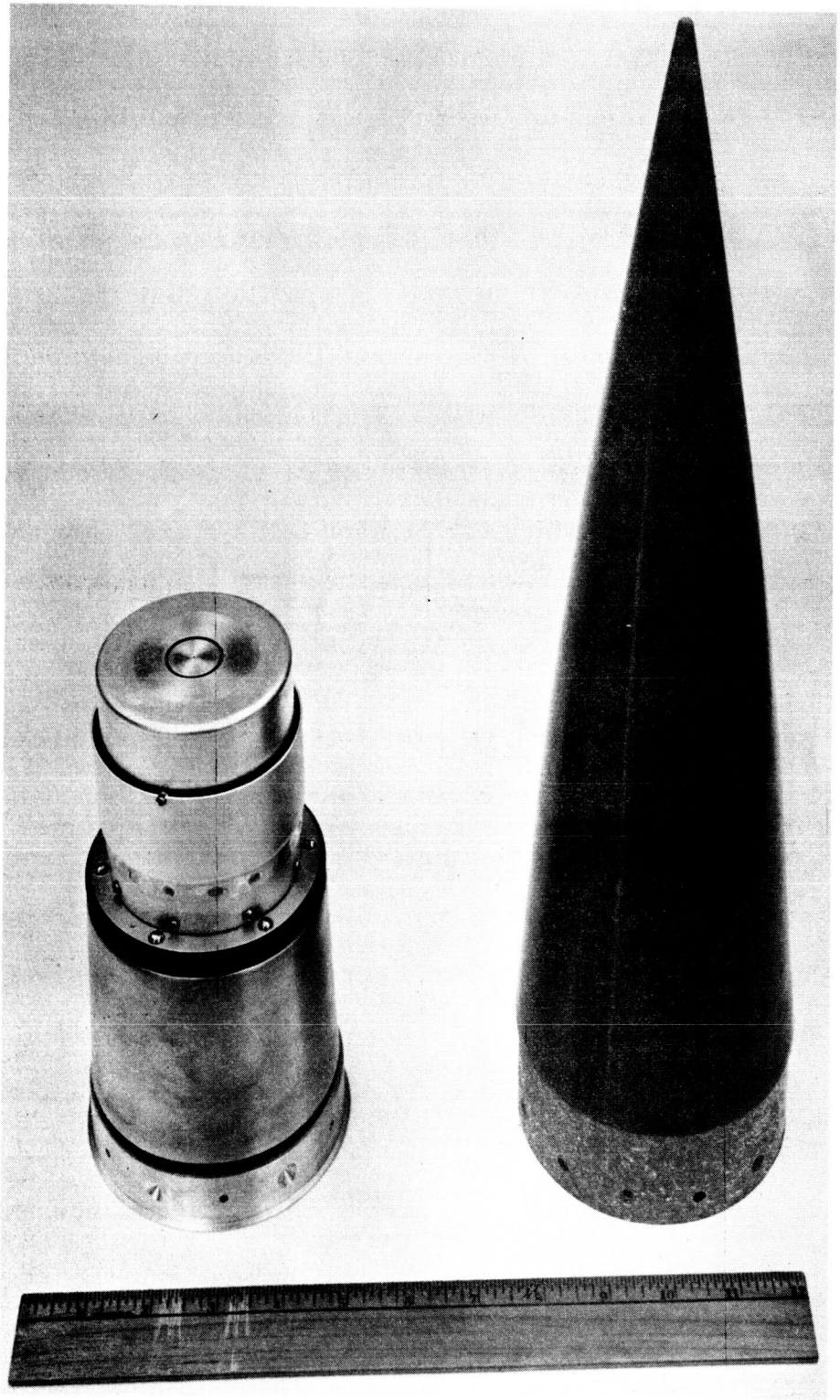

FIGURE 1 PROBE ASSEMBLY AND ARCAS NOSECONE

understood in theoretical terms. Because of the swinging of the parachute which usually takes place, angle of attack sensitive devices, which include the "Gerdien condenser", were discarded. A blunt geometry such as the one shown in Figure 1 is simple theoretically and shields the collecting surface from solar ultraviolet radiation. In addition, at altitudes higher than those considered in this paper, where free molecular flow prevails, probes of similar geometry have been used successfully by many workers, and for ion collection obey a simple ram collection theory with a consinusoidal dependence on angle of attack. Thus the possibility exists for developing a probe system, based on this geometry which can be used both for free flow and continuum measurements of charged particle densities.

IV. Probe Theory

One of the authors [2] (Hoult, 1965) has carried out a complete theoretical analysis of this probe for the case of high fixed potential operation of the collecting surface in the altitude range under consideration. This analysis is presented in Appendix I. The results of this analysis will be summarized here. The probe theory simplifies in the altitude range considered. These simplifications are:

(1) That the ionization density is low enough that the potential problem is governed by Laplace's equation ($\nabla^2 \phi = 0$).

(2) That the velocity of the probe, although not supersonic, is great enough so that convection of charged particles dominates drift and diffusion effects until well inside the boundary layer.

The first of these simplifications serves to completely uncouple the potential problem from the flow and charge transport problems.

The second simplification reduces the transport problem to one of knowing the electric field on the probe surface. It is shown that the principal component of current to a probe at high negative potential (a positive ion current) is given by the zero angle of attack ram current multiplied by a non-dimensionalized potential and divided by the diffusion Reynolds number. An additional correction factor of order of magnitude unity is necessary to account for the exact geometry of the probe (the relation of probe potential to the electric field at the collecting surface). For the geometry shown, this constant is $2/\pi$. Hence, for the probe geometry considered, the positive ion current to a highly negative probe is given by

$$I_+ = (e\, n^+ U \pi r^2)\left(\frac{2}{\pi}\right)\left(\frac{eV}{kT}\right)\left(\frac{1}{Rd}\right) \qquad (1)$$

where: n^+ is the number density of positive ions far from the probe, Rd is the diffusion Reynolds number (= UL/D, and U = free stream velocity, L = probe can diameter, D = ion diffusion coefficient). r is the radius of the collector, V is the probe potential, e is electron charge, T is temperature, and k is Boltzmann's constant.

A similar result can be derived for the current to a highly positive probe, which is primarily an electron current due to the high mobility of the electrons compared to negative ions.

A small negative ion current will reach the probe in both the high positive and high negative potential cases, but is too small to distinguish from the principal components of probe current by simple techniques. Initially, determination of negative ion densities will be done by subtracting measured electron densities from measured positive ion densities.

A simple way of looking at the results of the theory is that the viscous flow maintains a stagnant sample of the medium near the surface of the probe. Convection into this region maintains an ionization density not greatly different from the ionization density far from the probe. It can be shown that Equation (1) can be written

$$I_+ = en^+ \pi r^2 \mu_+ E_w \qquad (2)$$

where μ_+ is the positive ion mobility, and E_w is the electric field on the collecting surface.

It will be noted that these results are not sensitive to angle of attack.

V. Photo-Electric Effect on Probe Potential

In the case of a bipolar probe in a charged particle environment containing electrons and ions, it is well known that, if the probe surfaces have comparable area, the more positive electrode will acquire a slightly positive potential with respect to space potential and the more negative electrode will rise to a high negative potential. This is because the electrons which carry the current to the positive part of the probe have a much greater mobility than the ions which carry the current to the negative part of the probe. In effect a low impedance connection is provided between the positive electrode and the medium.

In the presence of solar radiation capable of producing photo electric currents, this situation may be drastically altered. The greater photo-current will flow to the less negative electrode, and this current will be carried by the high mobility photo-electrons. If this photo current is high enough, it may dominate the environmental effect described above.

The equilibrium situation may be with the more negative electrode near space potential, or even positive, and the more positive electrode at a positive potential giving a large electron current to balance the photo-current to the more negative electrode.

Although most of the solar ultra-violet radiation is absorbed above 80 km, radiation in the 2000-3000 Å range penetrates to the ozone layer. This radiation has been found by Bourdeau[3] and Whipple[4] to produce photo-electric currents of the order of 6×10^{-10} amp/cm^2 at 70 km and 3×10^{10} amp/cm^2 at 50 km. These currents were found not to be a strong function of the material used, being similar for tungsten and aluminum[4]. Using these photo-electric intensities along with photo-electron energy information obtained by Bourdeau[3] the equilibrium potentials of the probe geometry were estimated. With the probe collector can several volts negative with respect to the "return" can, which is the positive ion collection mode, it was found that the collecting potential did, in fact, remain large and negative above about 70 km. Between 70 km and 50 km the situation changed rapidly from charged particle domination to photo current domination, with the more negative electrode actually going positive at about 50 km. When the collecting electrode was more positive, the behavior of the potential was found to be less extreme. This calculation, along with the observation of an angle of attack dependence of current in a daytime experiment[5] not predicted by Hoult's probe theory, led to the conclusion that photo-electric effects could indeed control the potential of the probe. In order to check this hypothesis, a night experiment was conducted by Hale on March 21, 1965. No angle of attack dependence of probe current was observed. This confirmed the photo current hypothesis, and established

confidence in the probe theory.

In the future it will be necessary to take steps to eliminate or at least greatly reduce the effects of photo electric currents on potential. This may be accomplished by coating the sides of the probe can with material opaque to the solar radiation which produces photo-electrons. This also will aid in increasing the effective area ratio for charged particle collection between the return can and the probe can, which is sometimes necessary (particularly at night), in order to drive the probe sufficiently positive to measure electron densities. Ultimately, it may be desirable to increase the area ratio even further. This could be accomplished by an electrical connection from the return can to a metallized parachute.

VI. Error Analysis of Probe System

The most important source of error during daytime positive ion density measurements results from the uncertainty in probe potential which stems from the photo control of potential described in the previous section. This effect may lead to errors ranging from 10% at 70 km to 300% at 60 km. As previously stated, steps will be taken to reduce or eliminate this source of error.

The probe theory (Appendix I) assumes an incompressible medium. For the subsonic probe velocities typical for this system, this assumption is only partially justified. Estimates of compressibility effects lead to errors of about 25% at 70 km. to about 3% at 40 km. for a typical apogee (about 75 km). Work is currently in progress to determine the explicit dependence of number density upon Mach number, which will hopefully eliminate compressibility errors.

Equation (2) indicates that the quantity measured by this probe system is $n^+\mu_+$ (ion density times mobility) in the positive ion collection mode. Hence, in order to reduce the data to ion density data, the important quantity to be determined is μ_+, the positive ion mobility. Assuming the dominant positive ions in the D-region to be N_2^+, O_2^+, and NO^+ leads to an uncertainty in μ_+ of about 40% at the altitudes of interest. This error can be reduced only by more definitive mass spectroscopic measurements of D-region positive ion species coupled with more accurate determinations of the corresponding ionic mobilities in the laboratory.

A more complete examination of the error sources described above has been reported by Willis[5] (1965).

References

1 Hoult, D. P., "Weak Shock Waves in the Ionosphere", J. Geophys. Res., 69, 4617-4620, 1964.

2 Hoult, D. P., "D-Region Probe Theory", J. G. R. 70, 3182, 1965.

3 Bourdeau, R. E., Private communication.

4 Whipple, E. C., Jr., Private communication.

5 Willis, R. G., "A Subsonic Probe for the Measurement of D-Region Charged Particle Densities", Sci. Report No. 245, The Pennsylvania State University Ionosphere Research Laboratory, 1965.

Appendix I
D-Region Probe Theory
by D. P. Hoult

1. Introduction

This appendix presents the essential physics of the operation of a probe used to measure the number density of charged particles in the D region. The nose of a parachute borne blunt probe is charged to a potential and the current to a known area of the nose is measured. The probe is parachuted to produce subsonic flow [Hoult, 1964]. The significance of such an experiment is first, that positive and negative ions are not observable by ground based techniques, and second, the experimental determination of the number densities of positive ions, negative ions, and electrons is a necessary first step in understanding the complex chemical structure of the D region. The relationship between current, voltage, and the number densities of ions and electrons is required to interpret such data. Unfortunately, there is no existing probe theory for this purpose. For example, Lam [1964] assumes that the ratio of Debye length to body dimension is small, and ignores negative ions. The converse distinguishes the operation of a probe in the D region.

A typical probe dimension is 10 cm. velocity, 100 m/s; and voltage, 5v. This gives a Mach number of about 3/10, and the ratio of voltage to $\frac{kT}{e}$ (k = Boltzman's const, T = temp, e = electron charge) is about 2×10^2. At 50 km, the number density of neutrals $n(A_2)$ (A_2 stands for the chemically similar molecules NO, N_2, and O_2) is $10^{16}/cm^3$ at 80 km. The mean free path for neutral particles, Λ, is 10^{-2}cm at 50 km 1 cm at 80 km. Hence at 80 km the ratio of mean free path to

body dimension is 1/10, which is about the limit of a continuum theory. The number density of positive ions, $n(A_2^+)$ is about $10^3/cm^3$ and roughly constant with altitude. The number density of electrons, n(e) is about 10^3 at 80 km and $10^2/cm^2$ at 50 km. The gas is neutral so negative ions (here assumed to be A_2^-) make up the difference in charge density. The Debye length for electrons is 10 cm at 50 km and 3 cm at 80 km. Hence the ratio of Debye length to body dimension is 1 at 50 km; at 80 km this ratio is about 1/3. Due to the small concentration of charged particles in the flow, the fluid mechanical motion is unchanged by the ion collection process. For an incompressible flow (Mach number $<<$ 1) the Reynolds number, Re, ($= UL/\nu$, U = free stream velocity, L = probe dimension, ν = kinematic viscosity) is the important parameter. Re varies from 5×10^2 at 50 km to 10 at 80 km. Hence there is a laminar boundary layer over the probe.

The ratio of the change in velocity of a charged particle of mass m, accelerated for one mean free path by an electric field E due to a voltage on the probe of V, to the thermal speed v_o in the gas is

$$\frac{\Delta v}{v_o} \sim \frac{eE}{m} \left(\frac{\Lambda}{v_o}\right) \frac{1}{v_o} . \qquad (1)$$

Using $v_o \sim \sqrt{\frac{kT}{m}}$ and estimating $E \sim V/L$ gives

$$\frac{\Delta v}{v_o} \sim \left(\frac{eV}{kT}\right) \frac{\Lambda}{L} . \qquad (2)$$

If mobility is to have meaning, this ratio must be as small as say 10^{-1}. This gives an upper bound on the probe voltage of 2×10^{-2} volts at 80 km and 2 volts at 50 km. However, data on mobility [von Engel, 1955, fig. 61] in air show that this estimate is conservative by nearly a factor of 10^2, perhaps due to clustering. Thus the concept of mobility is appropriate up to altitudes near 80 km. By the principle of detailed balancing, the concept of diffusion is appropriate up to about 80 km also. The diffusion Reynolds number, Rd (= UL/D, where D = diffusion coefficient for positive or negative ions) is 10^3 at 50 km and 10 at 80 km.

In the next Section (Sec II) the nondimensional equations and boundary conditions are written down. It is shown that the density is so small, and the probe voltage so high (~5v) that the electric field is everywhere unchanged by the presence of the charged particles. Thus the electric field is that of the probe in a vacuum. Further, the region where positive ion diffusion is important, for a negatively charged probe, is much thinner than the thickness of the viscous boundary layer. Thus it happens that the positive ion current to a negative probe depends only on the electric field at the surface of the probe. For a positive probe, the same is true of negative ion and electron current. For a positive probe, the electron current always dominates the ion current by a factor β, the ratio of ion diffusion coefficient to electron diffusion coefficient. The effects of flow occur principally in determining the negative ion current to a negative probe. This current is very small compared to the positive ion current to a negative probe.

In the final section (Sec III) a sample calculation is presented to make explicit the general theory of section II. The flow over a disk,

normal to the free stream, is considered. The disk is charged to a fixed voltage and the current to a small area at the center of the disk is computed. The relationship between current, voltage and number densities is found.

II. The Governing Equations

The first approximation to subsonic flow is the incompressible case; the first correction is O(Mach number)^2. The incompressible approximation greatly simplifies the theory as the variation in mobility and diffusivity, and the effects of chemical reactions are all O(Mach number)^2. Due to the small concentration of charged particles, the fluid mechanical motion is unchanged by the ion collection process. Once the geometry of the probe, the Mach number ($<< 1$), and the Reynolds number, Re, are given, the flow velocity is (in principal) known.

Non-dimensionalize the flow velocity with U, the coordinates (x, y, z) with L, the potential with $\frac{e}{kT}$, and the charge density with the number density of electrons far from the body. Denote the nondimensional quantities as follows: $\vec{q}$ is the flow velocity, ϕ the potential, n^+ the positive ion density, n^- the negative ion density, and n^e is the electron density. Using this notation, and Einstein's relation, the equations are [Lam, 1964]

$$\alpha^2 \nabla^2 \phi = n^+ - n^- - n^e, \tag{1}$$

$$\nabla (Rd\, n^+ \vec{q} - n^+ \nabla \phi - \nabla n^+) = 0, \tag{2}$$

$$\nabla (Rd\, n^- \vec{q} + n^- \nabla \phi - \nabla n^-) = 0 \tag{3}$$

$$\nabla (\beta \, Rd \, n^e \vec{q} + n^e \nabla \phi - \nabla n^e) = 0, \tag{4}$$

where α is the ratio of Debye length to body dimension, and β is the ratio of ion to electron diffusion coefficients and is approximately the square root of the electron to ion mass ratio. The temperature of all charged particles is equal to the temperature of the neutrals (a good assumption in the altitude range under consideration).

Let λ be the ratio of negative ion density to electron density. Then the boundary conditions on charge density and potential far from the body are

$$n^+ = 1 + \lambda \tag{5}$$

$$n^- = \lambda \tag{6}$$

$$n^e = 1 \tag{7}$$

$$\phi = 0 \tag{8}$$

For an absorbing body, the number density of charged particles at the wall is zero. At the wall, the potential is known. Hence the boundary conditions at the wall read

$$n^+ = 0 \tag{9}$$

$$n^- = 0 \tag{10}$$

$$n^e = 0 \tag{11}$$

$$\phi = \phi_w \tag{12}$$

Since ϕ_w ($= \frac{eV}{kT}$, V = probe potential) is large, set

$$\phi = \phi_w \varphi(x, y, z) \tag{13}$$

Substituting 13 into 1 shows that the right hand side of 1 is at most $O(1/\alpha^2 \phi_w)$. Hence

$$\nabla^2 \varphi = 0 \tag{14}$$

is a first approximation to ϕ. Thus the electric field is that of a probe in vacuum. This is due to the very low number density of charged particles ($\alpha \sim O(1)$) and the high wall potential ($\phi_w >> 1$).

Consider a negative probe ($\phi_w < 0$). Let z be the normal to the wall. Using 14, and the fact that the flow is incompressible ($\nabla \cdot \vec{q} = 0$), equation 2 becomes

$$(Rd\, \vec{q} - \phi_w \vec{\nabla} \varphi) \cdot \nabla n^+ - \nabla^2 n^+ = 0 \tag{15}$$

For diffusion to be as important as convection, the last term in 15 must be as large as the effects of mobility ($-\phi_w \nabla \varphi \cdot \nabla n^+$). Following

the standard practice of boundary layer theory, set

$$\tilde{z} = \phi_w z. \tag{16}$$

Now if $\tilde{z}$ is of order one, the convection term in 15 is negligible, as the viscous boundary layer is $O(1/\sqrt{Re})$ thick which is $>> O(1/\phi_w)$, and as the velocity $\vec{q}$ is zero at the wall. Let the electric field at the wall be

$$\frac{\partial \phi}{\partial z} = - \phi_w f(x.y) \tag{17}$$

Then, for $\tilde{z}$ of order one, equation 15 becomes

$$- f(x,y) \frac{\partial n^+}{\partial \tilde{z}} + \frac{\partial^2 n^+}{\partial \tilde{z}^2} = O \tag{18}$$

The appropriate solution of 18 is

$$n^+ = (1 + \lambda)(1 - \exp + f(x,y)\, \phi_w z) \tag{19}$$

For a negative probe, $\phi_w < 0$. Thus 19 has the following properties: first, in the ion diffusion region, which is $O(\frac{1}{\phi_w})$ thick, 19 satisfies 18, the approximate form of 15. Second, outside of the ion diffusion region 19 satisfies 15, as n^+ is a constant for $\tilde{z}$ large. Thus 19 is the first approximation to n^+ everywhere.

In dimensional terms, the ion current to an area element dS of the probe surface is

$$dl = eD \left. \frac{\partial n (A_2^+)}{\partial Z} \right|_{wall} dS \qquad (20)$$

Using 19, this becomes

$$dl = e n_\infty (A_2^+) U dS \left(\frac{-\phi_w}{Rd}\right) f\left(\frac{X}{L}, \frac{Y}{L}\right) \qquad (21)$$

Thus the positive ion current to a negative probe is linear in potential.

For a positive probe, the electron density and negative ion density are found, by the same argument to be (note that $\phi_w > 0$)

$$n^e = 1 - \exp - f(x,y)\, \phi_w z \qquad (22)$$

$$n^- = \lambda \left(1 - \exp - f(x,y)\, \phi_w z\right) \qquad (23)$$

The electron and negative ion current to an area dS of a positive probe are

$$dl = e n_\infty (A_2^-) U dS \frac{\phi_w}{Rd} f\left(\frac{X}{L}, \frac{Y}{L}\right) + e n_\infty (e) U dS \frac{\phi_w}{\beta Rd} f\left(\frac{X}{L}, \frac{Y}{L}\right) \qquad (24)$$

Again this current is linear in potential. However, as $\beta \approx 5 \times 10^{-3}$ (approximately the square root of electron to ion mass ratio), the electron current always dominates the negative ion current. Hence it is impossible to measure negative ion current. Hence it is impossible to measure negative ion densities with a positive probe.

Note that use of a naive theory based on free molecular flow (current $\sim$ area x velocity x number density x charge), can be in error, from the data in the introduction, by a factor of 10 for positive ions and 10^2 for electrons.

The theory for positive probes is complete with equation 24, as the electron current completely dominates all other effects. For negative probes, the electron and negative ion densities must be discussed. Referring to equations 3,4, 13, and 14, it is seen that the effect of convection on electrons, $O(\beta Rd)$, is negligible compared to the effect of mobility $O(\phi_w)$ except very far from the probe. Electrons are stopped far from the probe. Hence the electron current to a negative probe is neglible. However the effects of convection on negative ions $O(Rd)$ can be larger than the effect of mobility $O(\phi_w)$. Hence negative ions are stopped near the probe, and the negative ion current may not be completely negligible. Explicit formulae for negative ion and electron densities, which depend on the detailed structure of the flow field, are worked out for the case of a disk in the next section. It is shown that the negative ion current is in fact very small.

III. A Charged Disk Normal to the Stream

Consider a disk of radius L normal to the free stream velocity. The flow is incompressible and axisymmetric. Let z be the (non-dimensional) direction normal to the disk, and the r the cylinder radius. The current collected inside $r = r_o \ll 1$ is measured. The relationship between the current to the collecting area, the voltage

applied and the number density of the media is to be found. Re, Rd, and ϕ_w are given. Hence the velocity field and potential field around the probe are known.

Define a stream function in terms of the fluid mechanical velocities as

$$\frac{\partial \psi}{\partial r} = - r q_z, \quad \frac{\partial \psi}{\partial z} = r q_r \tag{25}$$

As the collector is small ($r_o \ll 1$), only the velocity field and potential in the region near the axis ($r \ll 1$) are required. Outside the boundary layer, the stream function [Milne - Thompson, 1960] is, for $r \ll 1$,

$$\psi = + \frac{1}{2} r^2 + \frac{1}{\pi} (z - (1 + z^2) \cot^{-1} z) \left(\frac{r^2}{1 + z^2} \right) \tag{26}$$

The potential of a disk for $r \ll 1$ is [Jeans, 1925]

$$\phi = \phi_w \frac{2}{\pi} \tan^{-1} \left(\frac{1}{z} \right). \tag{27}$$

Using 17 and 27 thus gives, for $r \ll 1$,

$$f = \frac{2}{\pi} \tag{28}$$

By 21 and 28, the positive ion current to the collecting area of a negative disk is

$$I_+ = e\, n_\infty\, (A_2^+)\, U\, (\pi\, r_o^2\, L^2)\, \frac{2}{\pi}\, \frac{\phi_w}{Rd} \tag{29}$$

Likewise, the total current to the collecting area of a positive disk is approximately (the correction is O (β))

$$I_e = e\, n_\infty\, (e)\, U\, (\pi\, r_o^2\, L^2)\, \frac{2}{\pi}\, \frac{\phi_w}{\beta Rd} \tag{30}$$

Now consider the negative ion density, and electron density near a negative disk. The equations to be solved are 3 and 4 which take the form

$$(Rd\, \vec{q} + \phi_w\, \vec{\nabla}\, \varphi)\, .\, \nabla n^- - \nabla^2\, n^- = O \tag{31}$$

$$(\beta\, Rd\, \vec{q} + \phi_w\, \vec{\nabla}\, \varphi)\, .\, \nabla n^e - \nabla^2\, n^e = O \tag{32}$$

Near the axis the electric field and flow velocity in the radial direction are O(r). The z components of electric field and flow velocity have corrections which are O(r). Taking these facts into account, using the equations (31,32) and the boundary conditions (6, 7, 10, 11), it can be shown that near the axis the number densities behave as

$$n^- = n^-(z) + O(r^3) \tag{33}$$

$$n^e = n^e(z) + O(r^3). \tag{34}$$

Hence 33 and 34 reduce to

$$(\mathrm{Rd}\, q_z + \phi_w \frac{\partial \varphi}{\partial z}) \frac{dn^-}{dz} - \frac{d^2 n^-}{dz^2} = 0, \tag{35}$$

$$(\beta\, \mathrm{Rd}\, q_z + \phi_w \frac{\partial \phi}{\partial z}) \frac{dn^e}{dz} - \frac{d^2 n^e}{dz^2} = 0, \tag{36}$$

The error being O(r). Define Φ to be

$$\Phi = \int_0^z q_z \, dz. \tag{37}$$

Outside the boundary layer, Φ is the velocity potential. The solution of 35 and 36 satisfying the boundary conditions is

$$n^- = \frac{\lambda \int_0^z \exp(\mathrm{Rd}\,\Phi + \phi_w \varphi)\, dz}{\int_0^\infty \exp(\mathrm{Rd}\,\Phi + \phi_w \varphi)\, dz} \tag{38}$$

$$n^e = \frac{\int_0^z \exp(\beta\, \mathrm{Rd}\,\Phi + \phi_w \varphi)\, dz}{\int_0^\infty \exp(\beta\, \mathrm{Rd}\,\Phi + \phi_w \varphi)\, dz} \tag{39}$$

The corresponding negative ion and electron currents to the wall are in dimensional terms,

$$I_- = e \frac{n(A_2^-)\, U\, (\pi r_o^2 L^2)}{Rd} \left[\frac{e^{+\phi_w}}{\int_o^\infty \exp(Rd\ \Phi + \phi_w \varphi)\, dz} \right] . \quad (40)$$

$$I_e = \frac{e\, n_\infty(e)\, U\, (\pi r_o^2 L^2)}{Rd} \left[\frac{e^{+\phi_w}}{\int_o^\infty \exp(\beta Rd\ \Phi + \phi_w \varphi)\, dz} \right] . \quad (41)$$

For a negative disk, $\phi_w < 0$. Evidently the size of the currents is determined by evaluating the terms in brackets in 40 and 41. This is easily done by the method of steepest descent. [See Jeffreys and Jeffreys, 1956.] The results for the electron current are particularly simple. The integral in 41 can be approximated by an integral near the saddle point, which is found by setting the derivative of the exponent equal to zero. This gives, if the saddle point is located at $z = z_o$,

$$\beta Rd q_z(z_o) + \phi_w \frac{\partial \varphi}{\partial z}(z_o) = 0. \quad (42)$$

This equation locates the distance from the probe, z_o, at which the velocity due to mobility is equal and opposite to the flow velocity. This "stand off" distance, for electrons, is large:

$$z_o \tilde{=} \sqrt{-\phi_w / \beta Rd}. \quad (43)$$

By using 26, 27, 43 and the method of steepest descent, it can be shown that the electron current to the probe is of order

$$\exp \left\{ - \left| \phi_w \right| \quad + O \left(\sqrt{ - \phi_w / \beta Rd } \right) \right\} \tag{44}$$

and hence is completely negligible. Turning to the case for negative ions, one can say immediately that if the stand off distance is large, or even of order one, that the negative ion current is negligble. The only interesting case is to consider the stand off distance less than order one, but greater than the boundary layer thickness. In this case

$$z_o = \frac{-\phi_w}{Rd} \tag{45}$$

From the introduction, z_o is always greater than $O \left(\frac{1}{\sqrt{Re}} \right)$, which is the boundary layer thickness. Referring to equation 37, it is seen that the requirement that $z_o < 1$ means that convection dominates mobility effects until a region close to the wall is reached (the velocity is zero on the wall). Even in this case the negative ion current turns out to be very small compared to the positive ion current.

$$I_- = \frac{e\, n_\infty \, (A_2^-)\, U \, (\pi \, r_o^2 \, L^2)}{Rd^{3/2}} \; \pi \, e^{-\frac{2}{\pi} \phi^2 \, w/Rd} \tag{46}$$

In closing, note that currents of the form given by 29 or 30, by Einstein's relation, may be written in a form analogous to Gerdien condenser theory as

$$I \sim e\, n_{\infty} \text{ Area x mobility x electric field at wall.} \qquad (47)$$

Acknowledgments

The author wishes to thank Dr. L.C. Hale and Mr. R. Willis for many helpful discussions. The help of the Ionosphere Research Laboratory of The Pennsylvania State University is appreciated.

This work was supported in part by Grant DA-ARO-D-31-124-G537 and in part by NASA Grant NsG-134-61.

References

Hoult, D.P., 1964, Journal Geophys. Res. 69, 4617.

Jeans, 1925, The Math Theory of Electricity and Magnetism, Cambridge University Press, P. 249.

Jefferies, H. and Jefferies, B.S., 1956, Methods of Mathematical Physics, Cambridge University Press.

Lam, S.C., 1964, AIAA Journal 2, 256.

Milne-Thompson, L.M., 1960, Theoretical Hydrodynamics, MacMillian Company, New York, P. 476.

von Engle, A., 1955, Ionized Gases, Oxford at the Clarendon Press.

Appendix II
Probe Technology
by L. C. Hale

I. Introduction

A substantial body of technological development was necessary in order to conduct the probe experiments. Some of this technology is routine, some is believed to be unique and different. Complete circuit diagrams, along with discussion of the non-standard features of the circuitry, is presented in this appendix. Some of the pitfalls which required subsequent modifications are described. In cases where changes have been made, the currently used technique in described. A block diagram of the probe system electronics is shown in Fig. 2-1. The remainder of this appendix is devoted to the description of the elements in this block, and a description of the ground receiving equipment including data reduction equipment.

II. Current Measuring System

It is desired to measure as wide a range of current as possible consistent with the use of a reasonably simple system. To do this an operational feedback amplifier with a wide dynamic range is used in conjunction with automatic range switching circuit. This system provides a wide range of usable sensitivity for both positive and negative currents.

1. Feedback Electrometer

The heart of this circuit is the feedback electrometer of Fig. 2-2. (This circuit is based on one designed by L.C. Hale[1] and subsequently modified with the help of W. T. Homiller.)

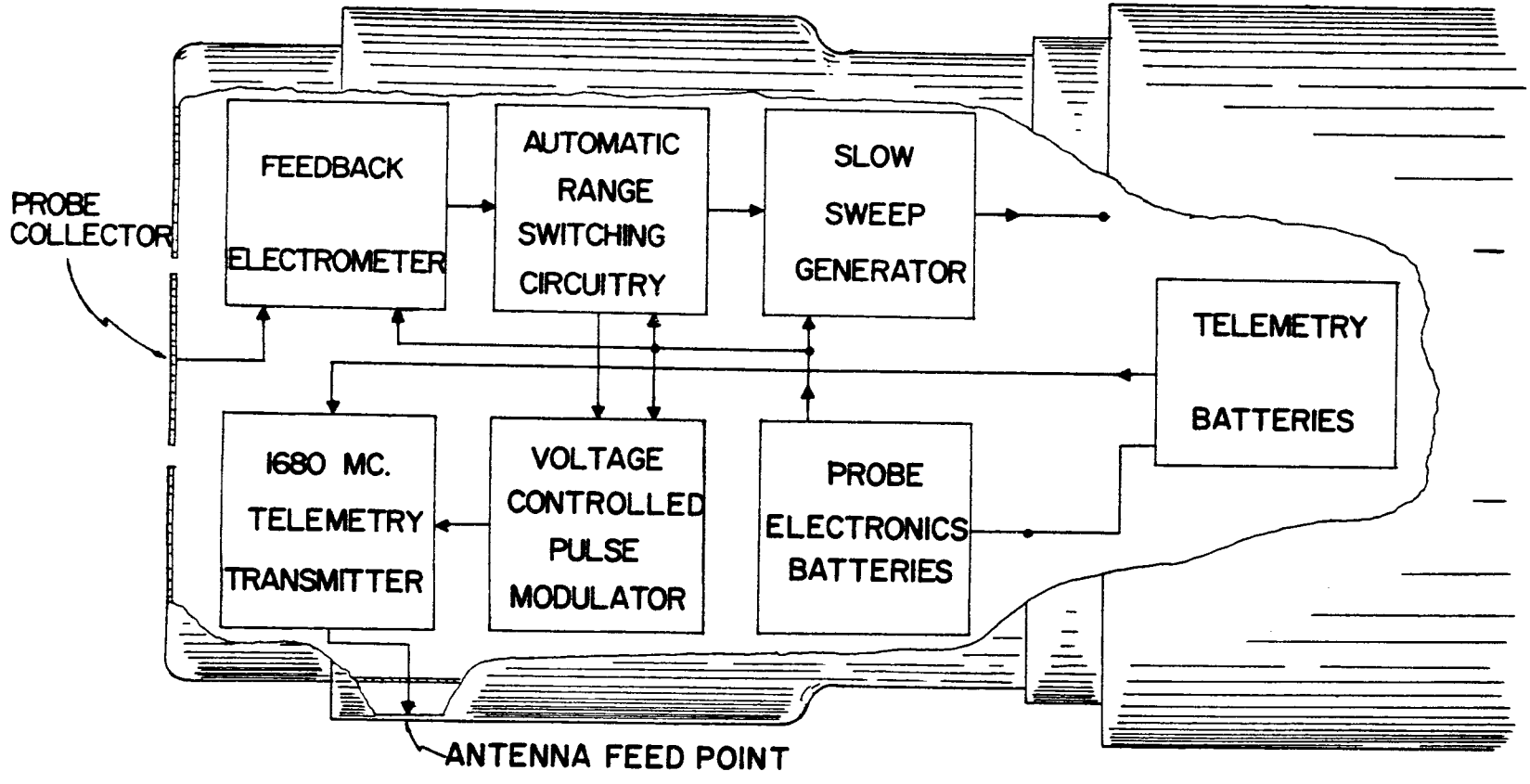

PROBE ELECTRONICS AND TELEMETRY

FIGURE 2-1

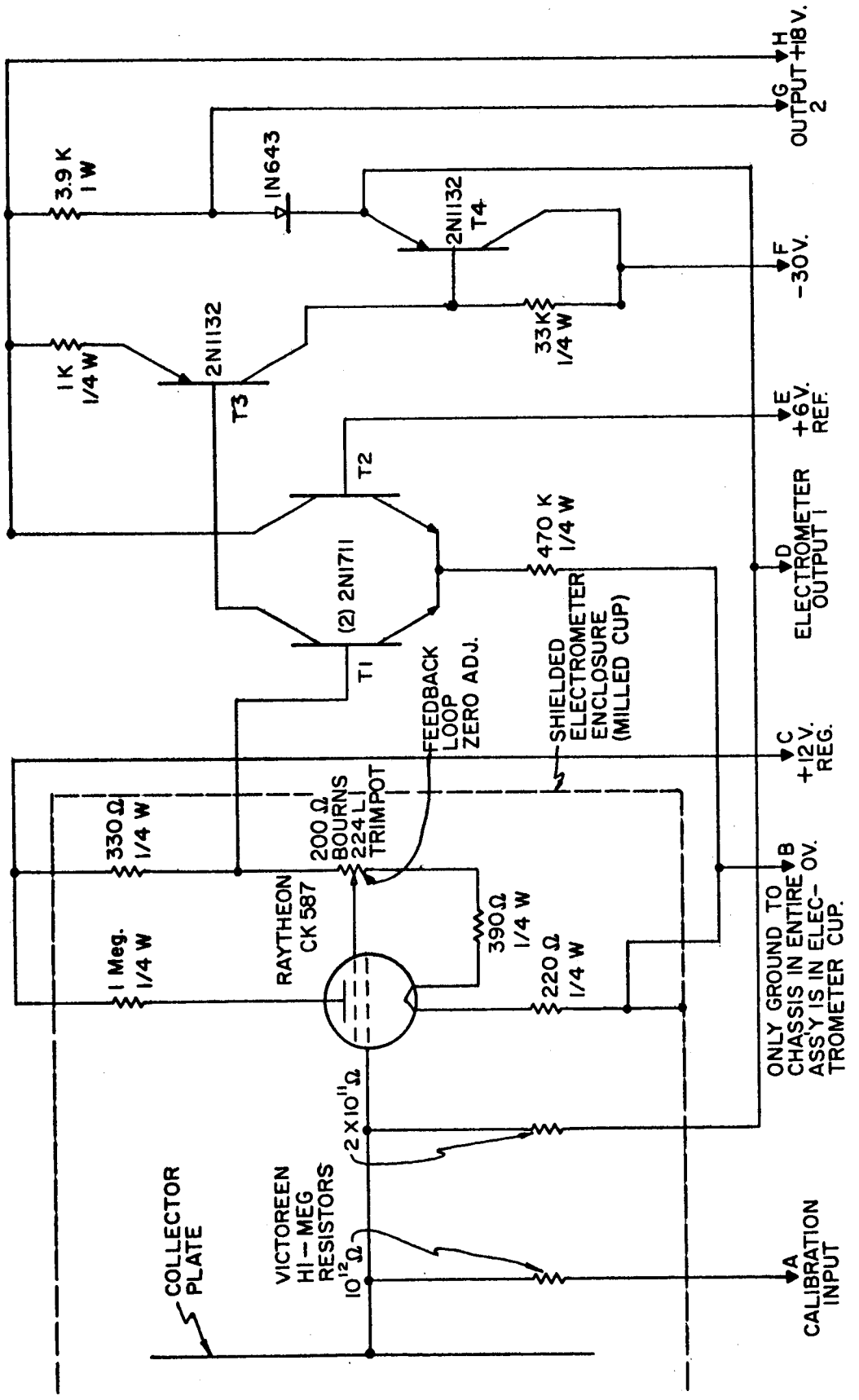

FIGURE 2-2 FEEDBACK ELECTROMETER

The advantages of operational feedback over a system without feedback are:

A. The high gain feedback loop holds the potential of the probe collector fixed near zero volts with respect to the guard can, essential if the probe potential is to be known accurately.

B. The frequency response is greatly improved. (The circuit shown is capable of better than 20 millisecond response time, or better than 10 ms. with the addition of a simple R-C corrective network in the feedback loop.)

C. The electrometer tube, a rather critical component, is held nearly fixed at an advantageous operating point under all operating conditions.

The electrometer is assembled in an aluminum cup which sits atop the electronics assembly, as shown in Fig. 2-3. All connections into this cup are made with the use of Erie Model 1250-003 Feed through RFI Filters, which were found necessary to prevent the telemetry RF from degrading the accuracy of the current measuring system. RF on the collector plate is prevented from contaminating the data by a filter made up of a coaxial capacitor and ferrite bead in the lead from the collector plate.

The sensitivity of the electrometer system shown is 2×10^{11} volts/amp. The circuit shown will operate linearly with an output of from +16 to -26 volts, corresponding to currents of -8×10^{11} to 13×10^{11} amperes. When used to drive a resistive load, the positive voltage swing is somewhat reduced, depending on the ratio of the load resistance to the emitter resistor of T4. The available swing in either

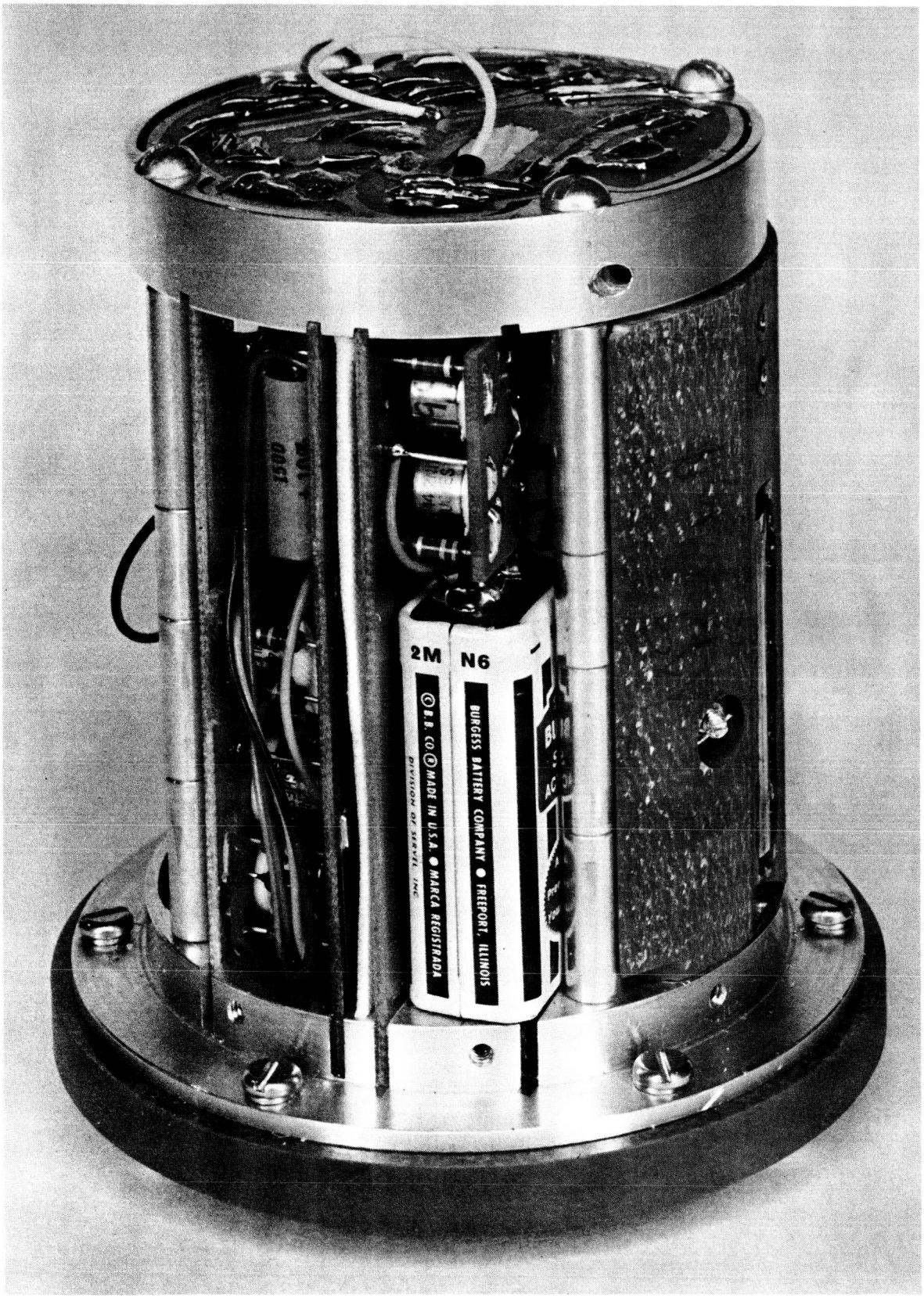

FIGURE 2-3 ELECTRONICS ASSEMBLY

direction can be increased simply by increasing the +18 or -30 volt supply voltage, subject to voltage breakdown ratings of transistors T3 and T4.

The stability of the feedback electrometer is good enough to permit additional d.c. amplification after the feedback loop. This additional gain provides a maximum usable sensitivity of about 10^{-13} amp.

III. Automatic Range Switching Circuitry

The automatic range switching circuitry shown in Fig. 2-4 provides five current ranges on the telemetry, the range in use being determined by the magnitude and sign of the input current.

With no signal input, the output of this circuitry is at about the middle of most sensitive range of operation, which is the output of a x7 d.c. amplifier following the electrometer feedback loop. As the signal is increased in either the negative or positive direction, the output is successively switched to the electrometer output (x1) and the attenuated electrometer output (x 1/7) sensitivity ranges. In addition, on the x1 and x 1/7 "positive" input ranges, level shifting is done to keep the telemetry input between 0 and +5 volts. The saturation output will depend on the d.c. voltages used to power the electrometer feedback loop output stages.

Identification of range is provided unambiguously by observation of the current waveform as the probe potential is swept from negative to positive. Since the current is a linear function of this potential it will always sweep most rapidly through the ranges as shown in Fig. 2-5, which shows the overall V-I curve of the current measuring system.

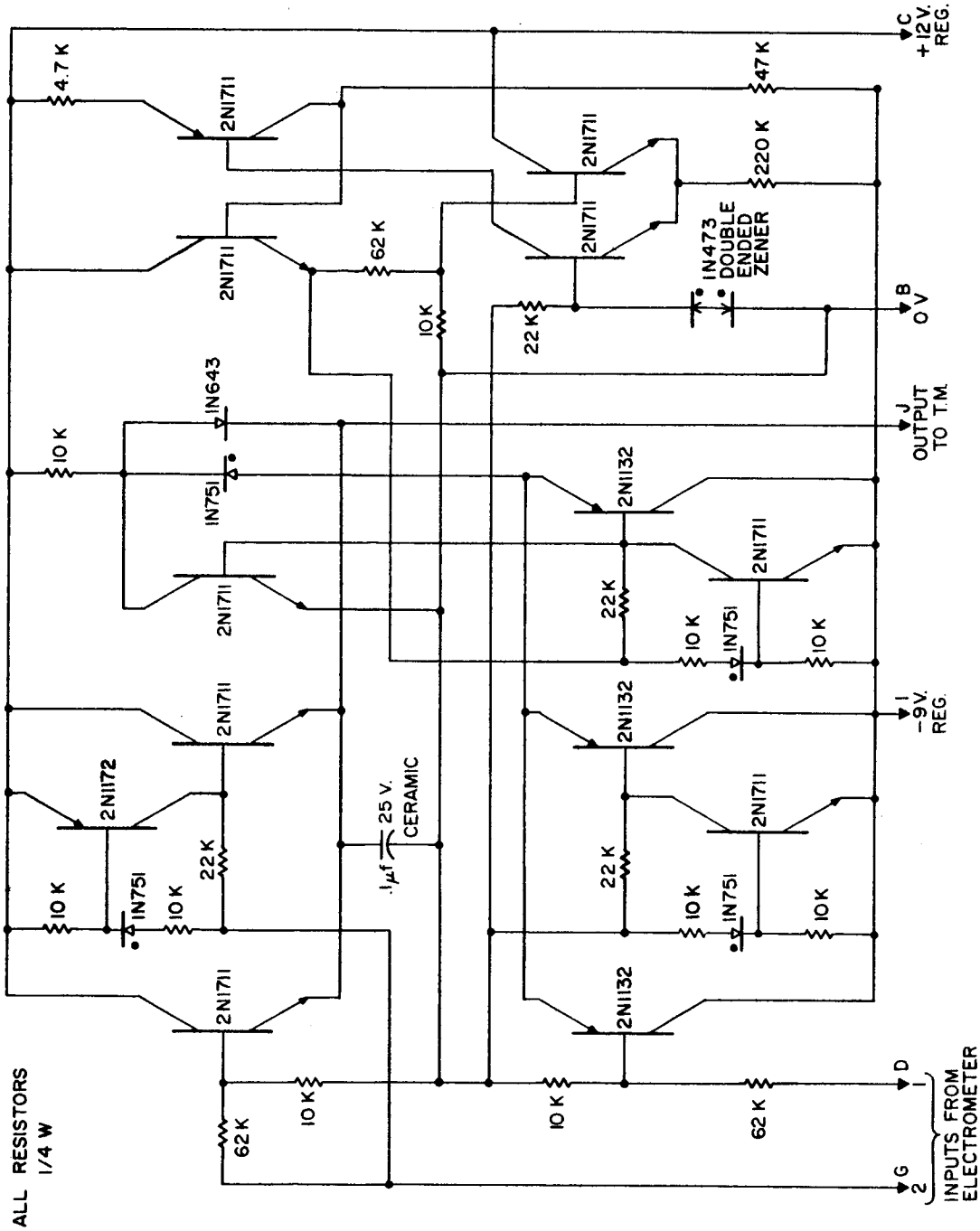

FIGURE 2-4 AUTOMATIC RANGE SWITCHING CIRCUITRY

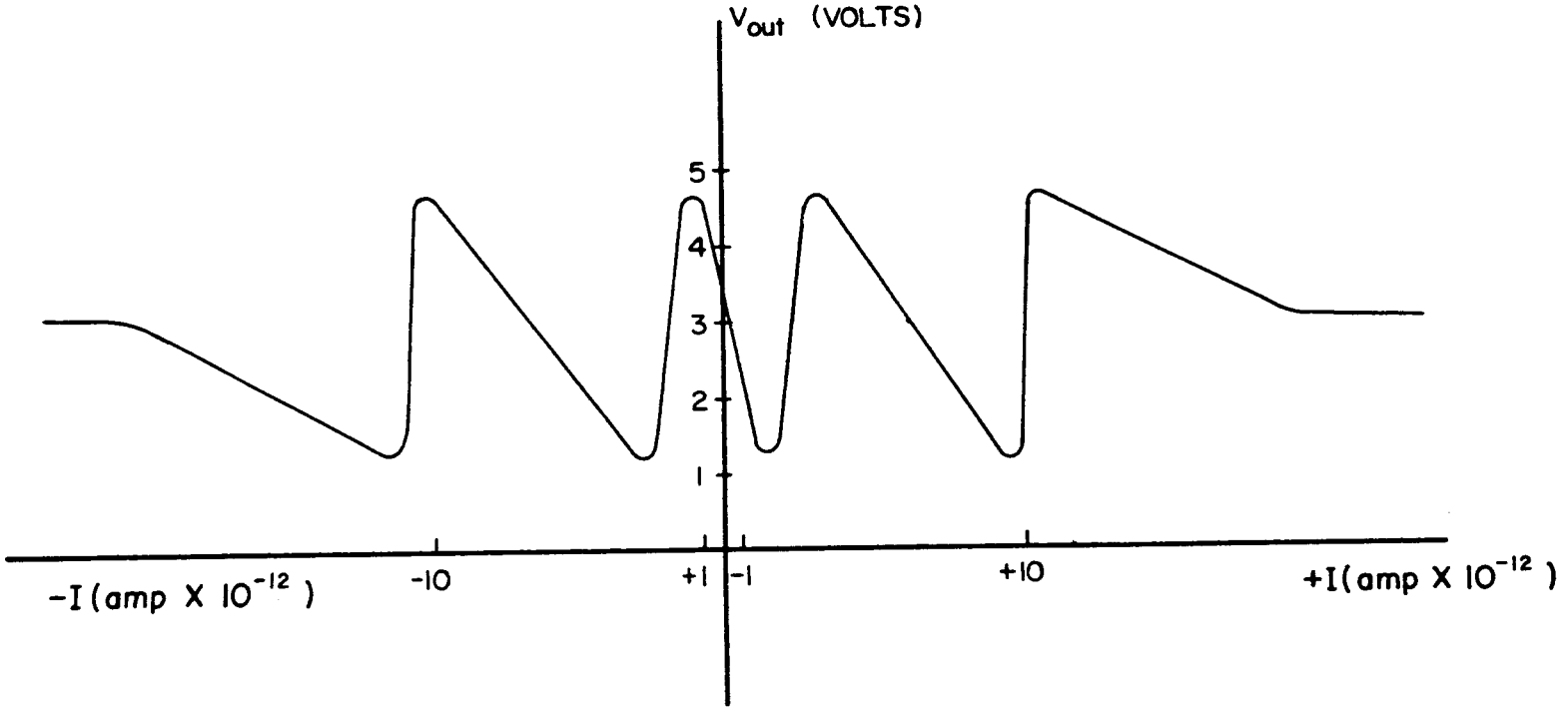

APPROXIMATE V-I CHARACTERISTIC OF ELECTROMETER AND RANGE SWITCHING CIRCUIT

FIGURE 2-5

Since it will always sweep most rapidly through the most sensitive range, identification of this range is unambiguous, and the other ranges may then be easily identified.

IV. Transmitter, Modulator, and Antenna System

The telemetry system makes use of the 1680 mc. integral tube and cavity transmitters which are used in "radiosonde" units used with weather balloons. These units provide in excess of one-half watt continuous output, and are adequately rugged and stable for use on the Arcas rocket.

Since the standard radiosonde receiving and recording system is the basic unit of the ground receiving equipment, it was decided to use a modulation system which is compatible with this system. The data is transmitted as a variable rate pulse modulation, with the pulse rate roughly linearly proportional to input voltage in the range of 20 to 200 pps.

The pulses are used to pulse the transmitter off for about 20μ sec. The system is then, characterizable as a form of PPM-AM, a system known for its good information efficiency. Ultimately, every interpulse interval is capable of conveying a meaningful 5 bit (3% accuracy) number. Thus, at about mid-channel (2.5 volts input to telemetry, 100 pps modulation rate) the information capacity of the system is about 400 bits/sec. This capacity is rarely used, but it is available, although special data reduction techniques are necessary to retrieve information at this rate. A description of data retrieval is given in the section on Ground Based Equipment.

The transmitter and voltage controlled blocking oscillator modulator are shown in Fig. 2-6.

The antenna, pictured in Fig. 1, is basically a .925λ x$^{\lambda}$/4x 1/8" slot, wrapped around the probe electronics can. It provides a relatively null free pattern and a VSWR (50Ω) at the feed point of about 2:1. (The VSWR may be made nearly unity, but this is not advisable, since the 1680 mc. cavity oscillators may cease oscillation when tightly coupled to a 50Ω load. This antenna is the subject of another report.[2]

The output coupling loop of the radiosonde transmitter is at anode potential. Accordingly, various transmission line and coupling schemes to provide d.c. isolation of the transmitter from the antennas were tried. These all could be made to work, but all required very careful individual adjustment for each payload, and frequently would not stay in adjustment.

The problem was solved by using a short direct connection of the transmitter to the antenna. The potential problem was solved by using a set of telemetry batteries completely separate from those powering the other electronic circuits, permitting operation of the telemetry filament supply at high negative potential, which makes possible "grounding" of the anode supply. This system has given good performance, with no need for adjustment except setting the frequency with the adjusting screw provided on the cavity oscillator.

V. Slow Sweep Generator, Power Supply, and Voltage Regulators

The sweep generator circuitry is shown in Fig. 2-7, along with the waveform generated. This waveform is applied to the battery or "return" can, hence the probe can voltage with respect to the return can

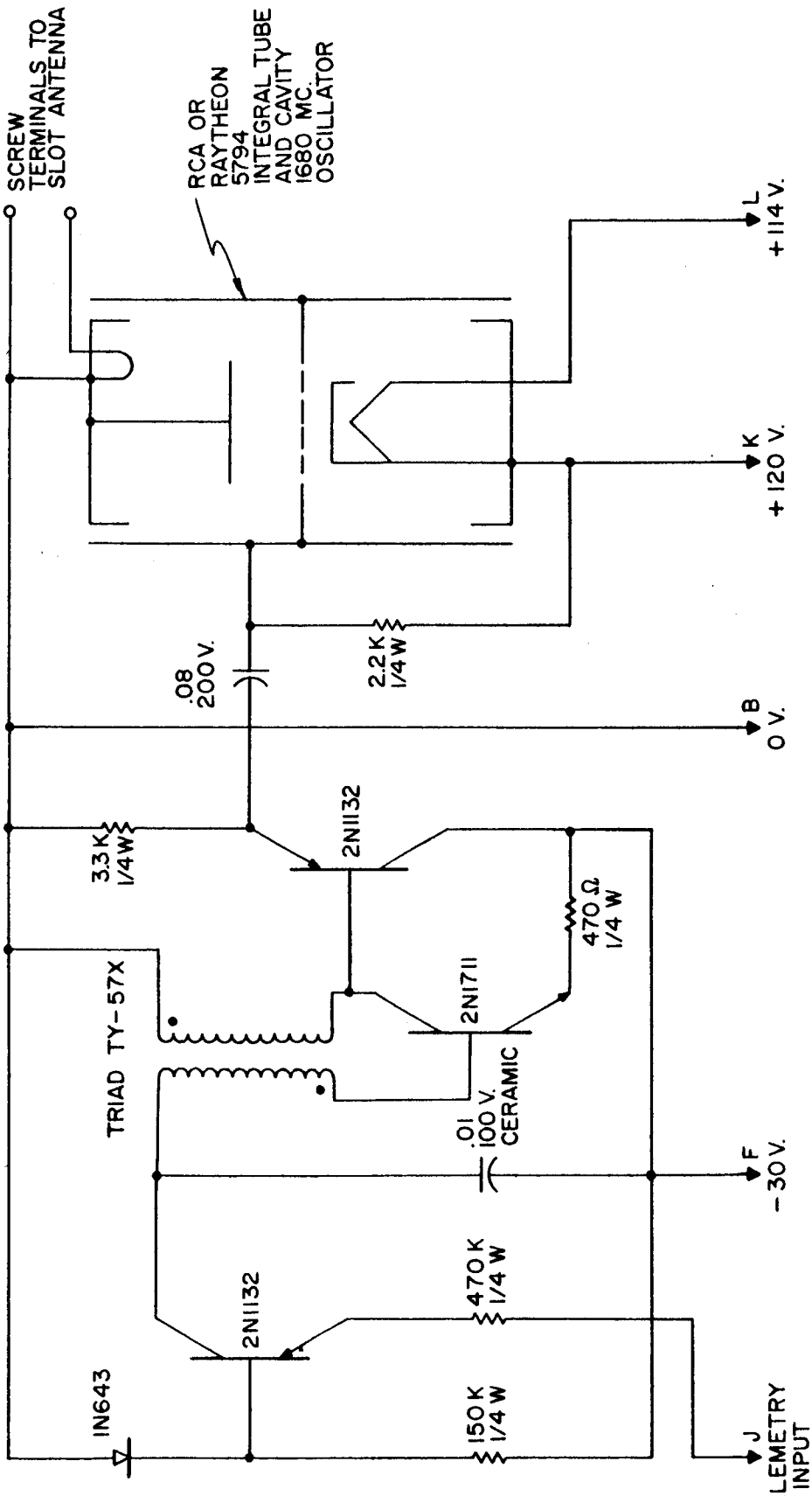

FIGURE 2-6 TELEMETRY TRANSMITTER AND MODULATOR

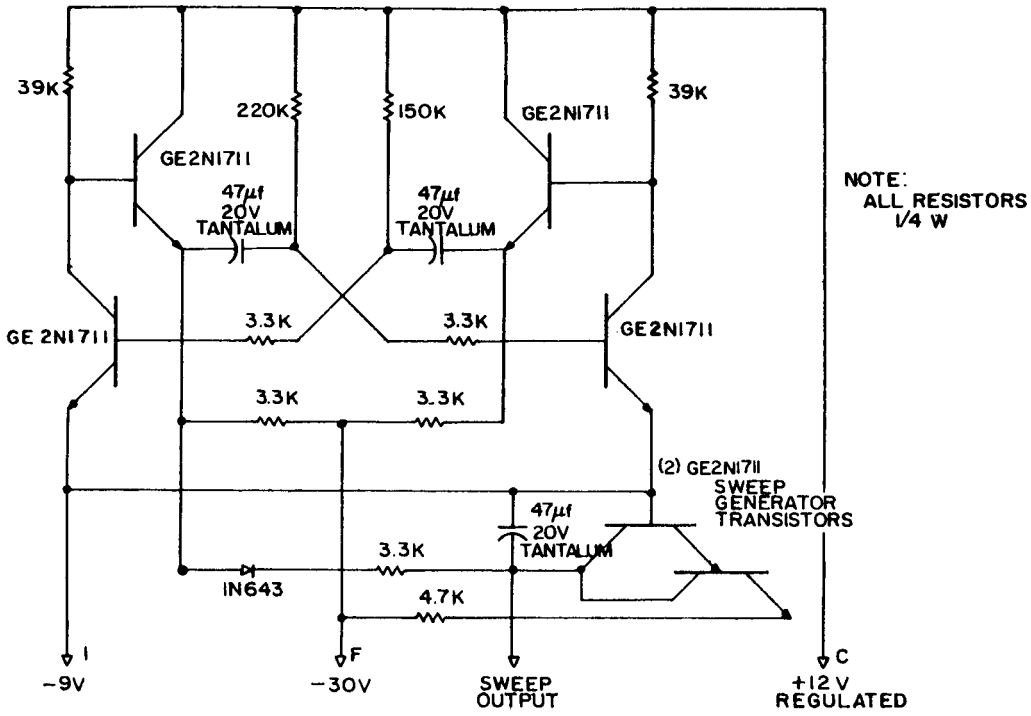

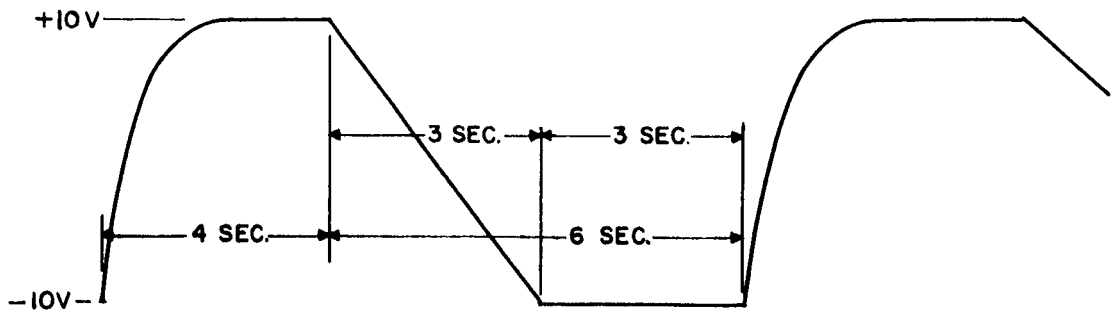

FIGURE 2-7 SWEEP GENERATOR AND SWEEP WAVEFORM

is given by the negative of this waveform. Thus during the period of fixed positive sweep potential positive ions are collected, and during the fixed negative potential period electrons are collected by the probe collecting disc. The probe electronics voltage regulators are shown in Fig. 2-8. The positive voltage regulator which supplies the electrometer tube uses a feedback circuit which provides one part in 10^4 regulation against supply voltage changes. The reference voltage from the 1N825A zener diode in this assembly is also used in the electrometer circuit. A single zener diode regulator provides an adequately regulated -9 volt supply.

The "return" can contains only the batteries which power the telemetry transmitter. All circuits are turned "on" by connecting the cable connectors which link the probe electronics to the telemetry batteries by utilizing appropriate jumper connections in the connectors.

VI. Ground Based Equipment

The telemetry signal is received on TMQ-5 (GMD) receiving equipment, designed for radiosonde balloon data acquisition. This system must be in near perfect operating condition, and preferably include a low noise preamplifier in order to receive good data from rocket altitudes. The TMQ-5 chart recorder is too slow for many purposes. For higher resolution data acquisition, the video output of the telemetry receiver is recorded, along with range time, on a 2 track tape. (A good "hi-fi" tape recorder, such as the Wollensak T-1580, is adequate for this recording.)

This tape is then played back through the system shown in Fig. 2-9,

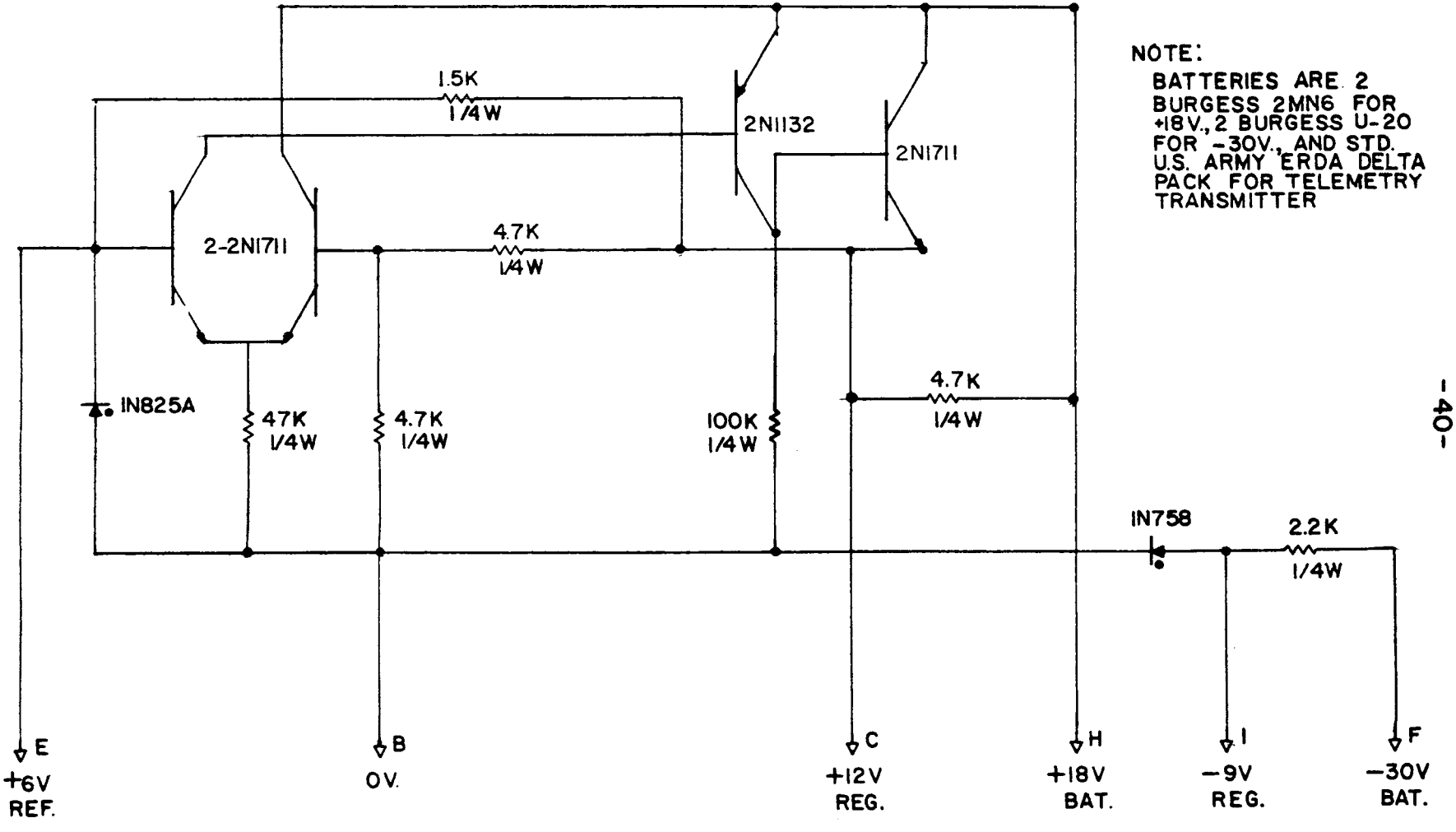

FIGURE 2-8 POWER SUPPLY VOLTAGE REGULATORS

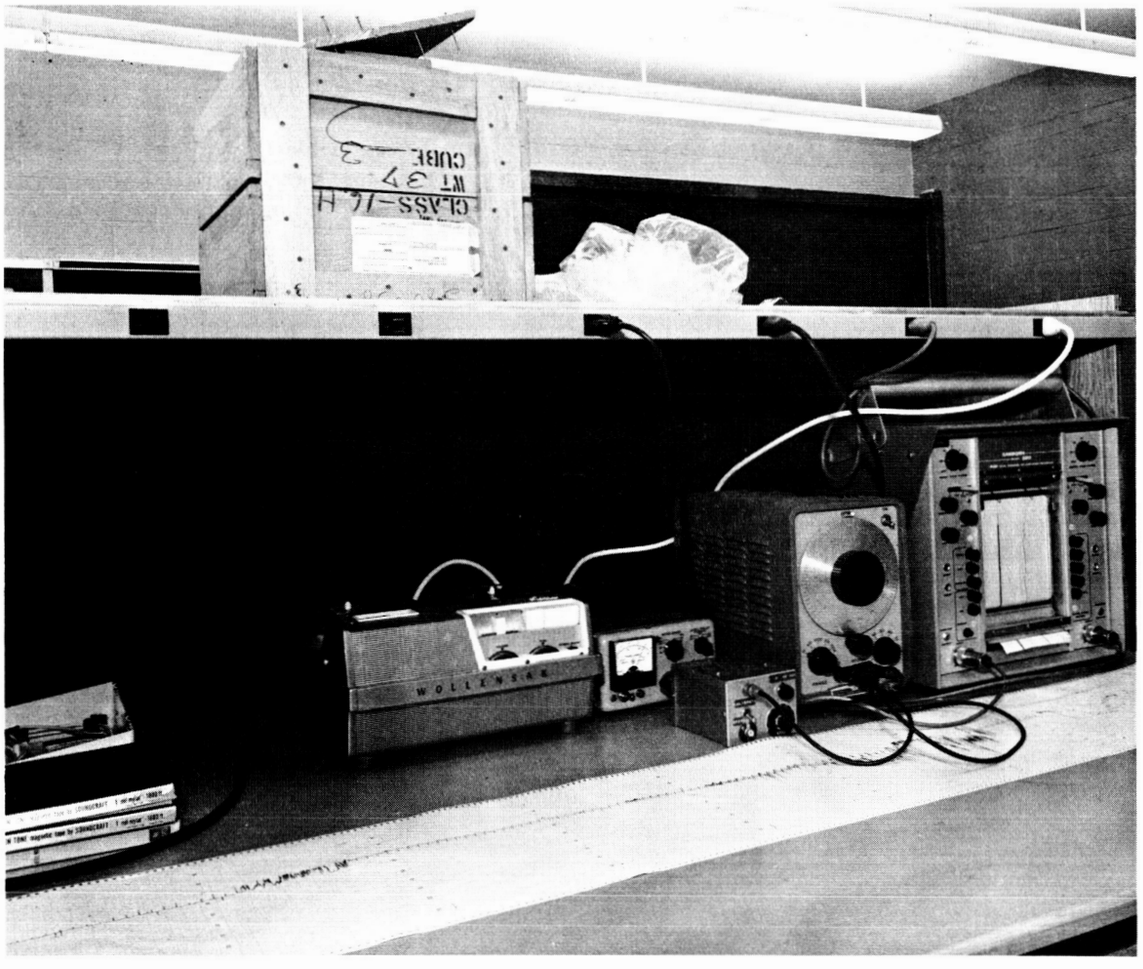

FIGURE 2-9 GROUND BASED EQUIPMENT

consisting of tape playback equipment (Wollensak T-1580 or T1515-4), data converter, and 2 track hot pen recorder. (Sanborn 320). The data converter is simply a transistorized "tachometer" (pulse rate to voltage converter), and a variable bandwidth low pass filter (1/5 to 10 cps), which can be used to obtain the best balance between noise free data and adequate frequency response. The circuit of the data converter is shown in Fig. 2-10. Reduction of data at higher rates can be accomplished, if needed, by manual reading of the interpulse intervals, recorded on a high speed data recorder. This has not proved to be necessary in any data reduction to date.

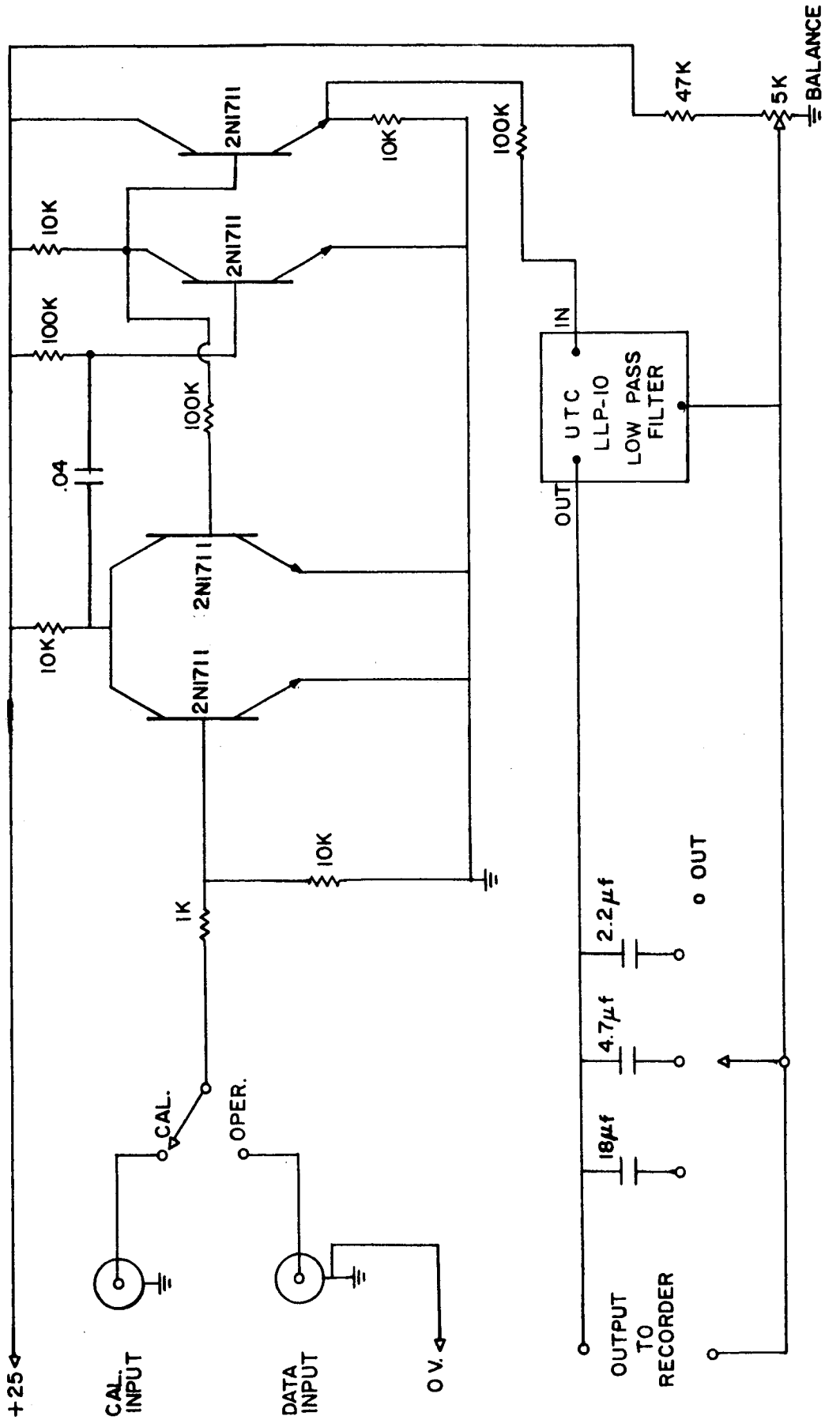

FIGURE 2-10 DATA CONVERTER

References

1. Hale, L. C., "A Probe Assembly for the Direct Measurement of Ionospheric Parameters", The Pennsylvania State University Ionosphere Res. Lab. Sci. Rep. No. 223(E), 1964.

2. Cuffin, N., "A Circular Slot Antenna for Use on Ionospheric Probes", The Pennsylvania State University Ionosphere Res. Lab. Sci. Rep. No. 249, 1965.